High-field magnetization process and spin reorientation in $(Nd_{1-x}Dy_x)_2Fe_{14}B$ single crystals

D. W. Lim, H. Kato, M. Yamada, G. Kido, and Y. Nakagawa
Institute for Materials Research, Tohoku University, 2-1-1 Katahira, Sendai 980, Japan
(Received 6 May 1991)

The high-field magnetization process in the $(Nd_{1-x}Dy_x)_2Fe_{14}B$ system has been investigated using single crystals with $x=0$, 0.125, 0.2, 0.33, 0.47, 0.6, and 1. Magnetization measurements were performed using steady magnetic fields of up to 300 kOe generated by a hybrid magnet system and pulsed magnetic fields of up to 400 kOe. When the field was applied along the [100] direction at low temperatures, the first-order magnetization process (FOMP) was observed in the samples with $x=0.125$, 0.2, and 0.33 as well as in $Nd_2Fe_{14}B$ ($x=0$). The field H_j where the FOMP occurred was found to increase rapidly with increasing x, reaching 320 kOe for the sample with $x=0.33$ at 4.2 K. The spin-reorientation temperature (T_{SR}), below which the magnetic moment tilted from the [001] to the [110] direction, was determined from ac susceptibility measurements. The T_{SR} decreased with increasing x. The tilting angle θ at 4.2 K also decreased gradually with increasing x. Magnetization curves of this mixed system were calculated by assuming the crystalline-electric-field parameters for the two end members. The observed concentration dependence of H_j and θ as well as the magnetization curves were successfully reproduced by this simple calculation.

I. INTRODUCTION

Since the Nd-Fe-B permanent magnet was discovered,[1] the magnetic and structural characteristics of the $R_2Fe_{14}B$ system (where R denotes a rare-earth element) have been extensively studied by many authors.[2-5] The $R_2Fe_{14}B$ compounds exhibit a variety of magnetic properties depending on R. The wide variety arises from the competition between the R-Fe exchange interaction and the crystalline-electric-field (CEF) interaction at the R sites. The high-field magnetization process in various $R_2Fe_{14}B$ single crystals has been studied systematically by present authors.[6] We have shown, for example, that the value of the saturation magnetization, in general, depends on the crystallographic direction along which the field is applied and that, in some light-R compounds, the hard-axis curve exhibits a jump in magnetization at high fields.[7] The latter was called the first-order magnetization process (FOMP).[8] All these observations have been systematically explained by the numerical calculations[6] based on a simplified Hamiltonian which takes, at each R site, the CEF and molecular field due to the R-Fe exchange interactions into account. The same method proved to be applicable to $R_2Co_{14}B$ system with $R=Pr$ and Nd,[9] although the main CEF term A_0^2 turned out to be evidently larger than that of $R_2Fe_{14}B$. A similar analysis in the $R_2Fe_{14}B$ system was made independently by Cadogan and co-workers;[10,11] the CEF and exchange parameters obtained are in good agreement with ours, although there is a slight discrepancy between the two results. We have reported more recently the detailed investigation of the high-field magnetization process in diluted systems $(Nd_{1-x}R_x)_2Fe_{14}B$ with $R=Y$ and La.[12] The diluted systems show a decrease in both spontaneous magnetization M_0 and jump field H_j with increasing x.

In order to get further information about the CEF potentials and R-Fe exchange interactions, we have extended our investigations to the $(R_{1-x}R'_x)_2Fe_{14}B$ system, where both R and R' are magnetic rare-earth ions. It has already been found that the substitution of Dy or Tb for Nd in $Nd_2Fe_{14}B$ results in an increase in magnetic anisotropy and a decrease in magnetization.[13] The latter is due to ferrimagnetic coupling between Fe moments and Dy or Tb moments, whereas Nd moments are ferromagnetically coupled with Fe moments. On the other hand, the most interesting are the variations of the FOMP and spin reorientation by partial substitution of Dy for Nd, since the occurrence of FOMP is dominated by the delicate balance of the CEF potentials and R-Fe interactions.

In this paper we will report the experimental results of high-field magnetization process in $(Nd_{1-x}Dy_x)_2Fe_{14}B$ single crystals and compare them with the calculations by extending the Hamiltonian so as to deal with the mixed $(R_{1-x}R'_x)_2Fe_{14}B$ system. Results of ac susceptibility measurements, which were performed to determine the spin-reorientation temperature precisely, are also presented.

II. EXPERIMENT

Single crystals of $(Nd_{1-x}Dy_x)_2Fe_{14}B$ with $x=0$, 0.125, 0.2, 0.33, 0.47, 0.6, and 1 were grown with a floating-zone method under purified argon-gas atmosphere using an infrared imaging furnace. Final concentration of the substitutional element x was not traced; the value x represents the nominal concentration. The deviation in x is, however, supposed to be small enough since the magnetic properties of the single crystals are consistent with those of polycrystalline alloys with precise values of x. We have not checked whether there exists any site preference of the two rare-earth elements. We expect that it is

not significant, since the experimental results are well explained by a calculation which assumes a random substitution of Dy for Nd, as will be shown below. The crystal was embedded into a cube of epoxy resin so that the principal crystallographic axes became parallel to cube edges. The crystallographic axes were determined by Laue x-ray Polaroid photographs.

Magnetization measurements were carried out by a sample extraction method in steady magnetic fields of up to 300 kOe generated by a hybrid magnet system at High Field Laboratory, Tohoku University.[14] The demagnetizing field was corrected by assuming a spherical geometry. For measurements in higher fields, a pulsed-magnet system with induction method was employed, although the magnetization value obtained was less accurate than that in steady fields.

The low-field ac susceptibility χ_{ac} was measured as a function of temperature using a mutual inductance Hartshorn bridge method. The 85-Hz ac magnetic field with the amplitude of 0.1 Oe was applied parallel to the [110] direction of the sample. The sample temperature was monitored by a thermocouple of Au(Fe) versus normal silver. The spin-reorientation temperature T_{SR} was obtained from a cusp temperature of χ_{ac}.

III. RESULTS

Magnetization curves of $(Nd_{1-x}Dy_x)_2Fe_{14}B$ single crystals along the [001], [100], and [110] directions at 4.2 K are shown in Fig. 1, together with the calculated curves which will be discussed later. For the sample with $x=1$ ($Dy_2Fe_{14}B$), we extended the maximum field up to 300 kOe in the present study, while that of previously reported curves[6] was limited to 150 kOe. Magnetization values of easy- and hard-axis directions are seen to become almost equal around 300 kOe. In the compounds with small x, the magnetization curves along the [100] direction exhibit the FOMP as observed in $Nd_2Fe_{14}B$[7]. The jump field H_j, where the FOMP occurs, increases rapidly with increasing x, being 160 kOe for $x=0$ and 320 kOe for $x=0.33$. The latter result was obtained by the pulsed-field measurement. The easy direction of magnetization of all samples except for $x=1$ is tilted from [001] toward [110] at 4.2 K, since the magnetization in the (001) plane has a finite value in zero field.

Figure 2 shows the concentration dependence of the jump field H_j, the magnitude of discontinuity of magnetization ΔM at H_j, the spontaneous magnetization M_0, and the zero-field tilting angle θ at 4.2 K. The solid lines in Fig. 2 are the calculated results, which will be discussed in the next section. It is clearly seen that, with increasing x, H_j increases rapidly, while ΔM decreases significantly. The value of M_0, deduced from the zero-field magnetization values of the [001] and [110] directions, decreases linearly with increasing x, as expected from a simple picture of this mixed magnetic system. For small values of x, the decrease of θ is rather gradual in contrast with the rapid change in H_j and ΔM. It should be noted that the zero-field properties such as M_0 and θ are not so sensitive to x, while the Dy substitution has a drastic influence on the high-field properties related to FOMP.

Magnetization curves at 290 K are shown in Fig. 3, together with the calculated curves which will also be discussed later. These curves reveal that the anisotropy field H_A^*, where the hard-axis magnetization reaches the saturation, is obviously enhanced with increasing x. The concentration dependence of H_A^* is presented in Fig. 4(a). It is shown that H_A^* increases drastically with increasing x, evidently related to the very high uniaxial anisotropy of Dy ions. In $Dy_2Fe_{14}B$ ($x=1$) the hard-axis magnetization curve does not show the tendency of saturation even at the field of 270 kOe, as seen in Fig. 3. An interesting

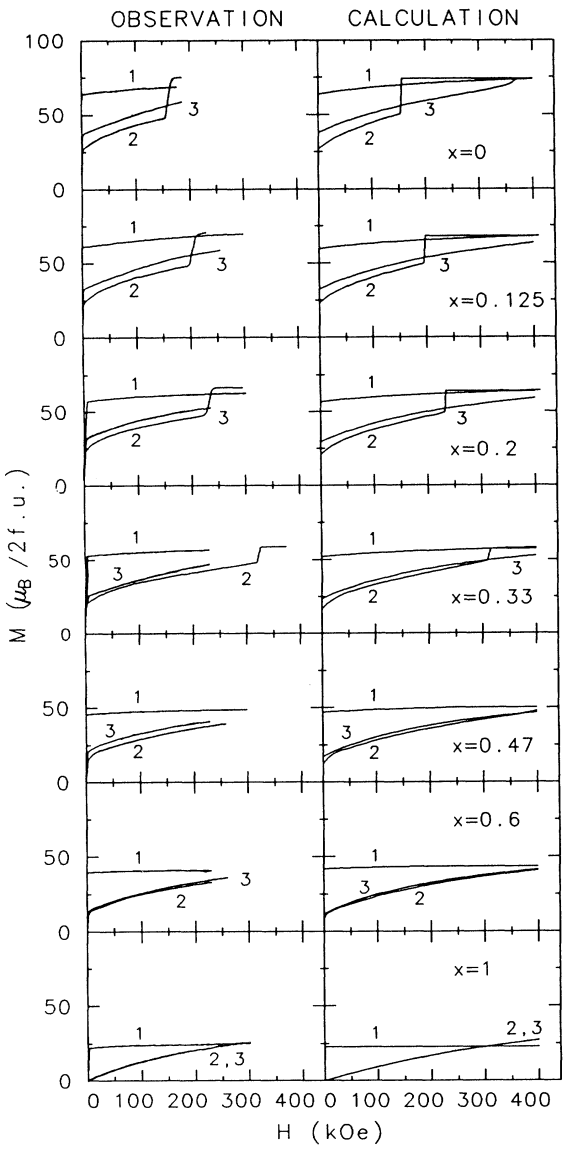

FIG. 1. Observed and calculated magnetization curves of $(Nd_{1-x}Dy_x)_2Fe_{14}B$ single crystals at 4.2 K. The numbers 1, 2, and 3 in the figure denote that the external field is applied along the [001], [100], and [110] directions, respectively.

feature of the room-temperature curves is the concentration dependence of difference in the saturation magnetization M_s between the [001] and [100] directions, as shown in Fig. 4(b), in which M_s is defined as the magnetization at H_A^*. The solid and dashed lines in Figs. 4(a) and 4(b) show the result of calculation, which will be mentioned later. In the case of $Nd_2Fe_{14}B$ ($x=0$), the saturation magnetization of the easy direction is about 3% larger than that of the hard direction. This is due to the CEF interaction, which causes the contraction of Nd moment in the hard direction. A similar behavior is also observed in the sample with $x=0.125$, although the difference is very small. For the $x=0.33$ sample, on the other hand, the magnetization values of easy and hard directions become equal around 140 kOe, and at higher fields the latter value rather exceeds the former. Such an intersection of the two curves becomes more evident for the samples with $x \geq 0.47$, as can be seen in Fig. 3. The reason for the larger saturation value in the hard direction is the contraction of the Dy moments, which are coupled ferrimagnetically to the Fe moments.

The temperature dependence of the ac susceptibility for the samples with various Dy concentrations is shown in Fig. 5. The ac field is applied along the [110] direction. The cusp temperature of each curve corresponds to the spin-reorientation temperature T_{SR}, at which the response of magnetic moment to the external field should be maximum. Our T_{SR} value obtained for the sample with $x=0$ is 126 K, which is lower than the value of 135

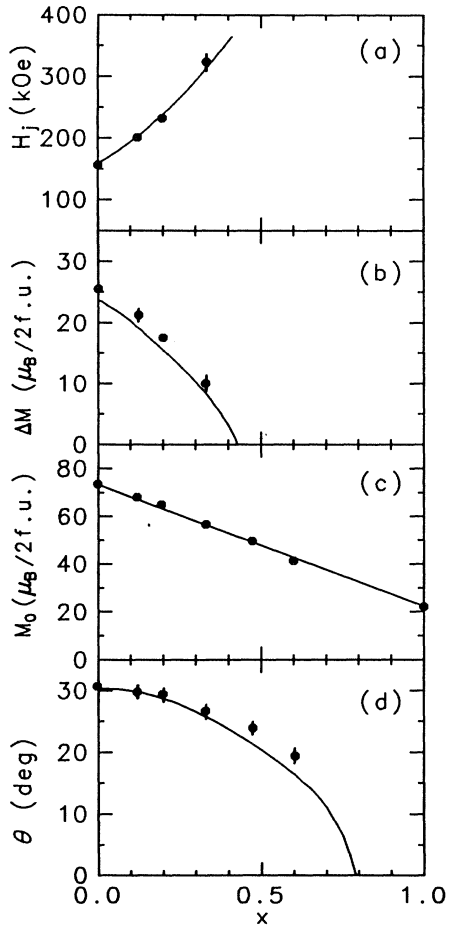

FIG. 2. Concentration dependence of (a) the jump field H_j where the FOMP occurs in the [100] direction, (b) the discontinuity of magnetization ΔM at H_j, (c) the spontaneous magnetization M_0, and (d) the tilting angle θ for $(Nd_{1-x}Dy_x)_2Fe_{14}B$ single crystals at 4.2 K. Solid curves are corresponding calculations as described in text.

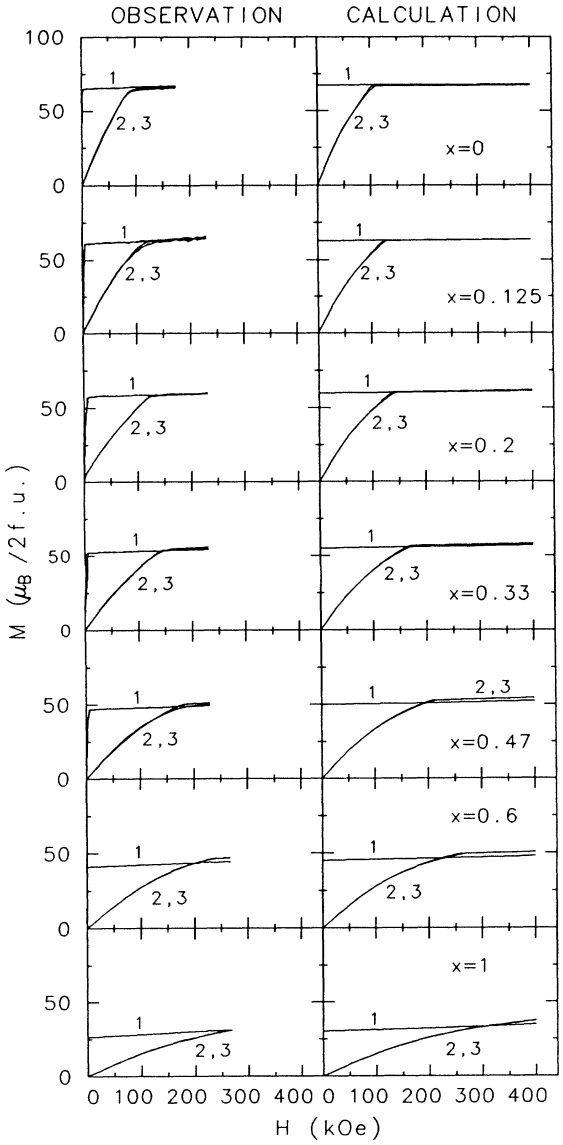

FIG. 3. Observed and calculated magnetization curves of $(Nd_{1-x}Dy_x)_2Fe_{14}B$ single crystals at 290 K. The numbers 1, 2, and 3 in the figure denote that the external field is applied along the [001], [100], and [110] directions, respectively.

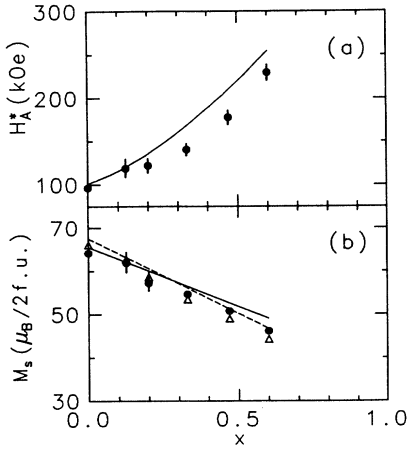

FIG. 4. Concentration dependence of (a) the anisotropy field H_A^* and (b) the saturation magnetization M_s in the easy [001] direction (△) and hard [100] direction (●) for $(Nd_{1-x}Dy_x)_2Fe_{14}B$ single crystals at 290 K. A solid line in (a) shows the calculated values for H_A^*. Dashed and solid lines in (b) show the calculated values for M_s[001] and M_s[100], respectively.

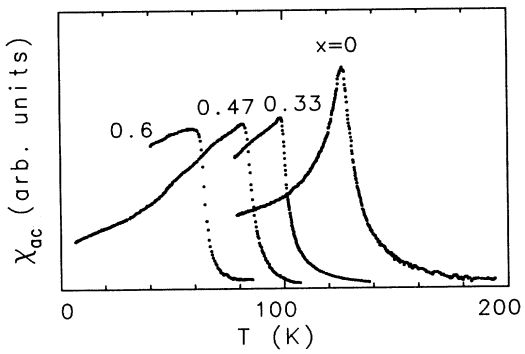

FIG. 5. Temperature dependence of the ac susceptibility of $(Nd_{1-x}Dy_x)_2Fe_{14}B$ single crystals with the ac magnetic field applied along the [110] direction.

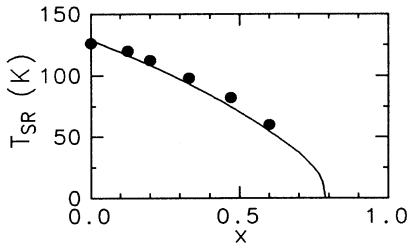

FIG. 6 Concentration dependence of the spin-reorientation temperature for $(Nd_{1-x}Dy_x)_2Fe_{14}B$ single crystals. A solid curve exhibits the calculated result.

K originally reported by Givord, Li, and de la Bathie.[4] Ibarra *et al.*,[15] on the other hand, have given the value 126±1 K using the ac susceptibility measurement on the polycrystalline sample, which is in accordance with our result. The T_{SR} is plotted against x in Fig. 6, showing a gradual decrease with increasing x. The solid line in the figure is the result of calculation which will be discussed below.

IV. ANALYSIS AND DISCUSSION

In order to analyze the magnetization process in the mixed $(Nd_{1-x}Dy_x)_2Fe_{14}B$ system, we extend the simple formalism of the calculation in $R_2Fe_{14}B$ (Ref. 6) to this mixed $(R_{1-x}R'_x)_2Fe_{14}B$ system. It was proved to be a good assumption that the R-R exchange interaction in $R_2Fe_{14}B$ is negligibly weak when it is compared with the R-Fe interaction and Fe-Fe interaction. This assumption will also be applied to the mixed $(R_{1-x}R'_x)_2Fe_{14}B$ system. Thus we assume that the total free energy at temperature T in the external field $\mathbf{H}$ in the system of $2(R_{1-x}R'_x)_2Fe_{14}B$ is simply expressed as

$$F(\mathbf{H},T)=-(1-x)k_BT\sum_{i=1}^{4}\ln Z(i)-xk_BT\sum_{i=1}^{4}\ln Z'(i)+28K_{Fe}(T)\sin^2\theta_{Fe}-28\mathbf{m}_{Fe}(T)\cdot\mathbf{H}\ , \quad (1)$$

where the last two terms are, respectively, the anisotropy energy and Zeeman energy of the Fe sublattice, K_{Fe} is the uniaxial anisotropy constant per Fe ion, and θ_{Fe} is the angle between the c axis and direction of Fe magnetic moment $\mathbf{m}_{Fe}$. The first and second terms are contributions from R and R' ions, respectively, where $Z(i)$ and $Z'(i)$ are partition functions defined from the sth eigenvalues $E_s(i)$ and $E'_s(i)$ of the Hamiltonians $\mathcal{H}_R(i)$ and $\mathcal{H}_{R'}(i)$ for the ith R and R' ions ($i=1$, 2, 3, and 4, corresponding to f_1, f_2, g_1, and g_2 sites, respectively):

$$Z(i)=\sum_s \exp[-E_s(i)/k_BT]\ , \quad (2)$$

$$\mathcal{H}_R(i)=\lambda\mathbf{L}\cdot\mathbf{S}+\mathcal{H}_{CEF}(i)+2\mu_B\mathbf{S}\cdot\mathbf{H}_m(i)+\mu_B(\mathbf{L}+2\mathbf{S})\cdot\mathbf{H}\ , \quad (3)$$

and the corresponding equation for $\mathcal{H}'_R(i)$ with λ', $\mathbf{L}'$, $\mathbf{S}'$, $\mathcal{H}'_{CEF}(i)$, and $\mathbf{H}'_m(i)$. Here $\mathbf{H}_m(i)$ and $\mathbf{H}'_m(i)$ are molecular fields acting on the R and R' ions at the ith site due to the R-Fe and R'-Fe exchange interactions, respectively. The second term of Eq. (3) is the CEF Hamiltonian expressed as

$$\mathcal{H}_{CEF}(i)=A_2^0(i)\sum_j(3z_j^2-r_j^2)+A_2^{-2}(i)\sum_j 2x_jy_j+\cdots+A_6^{-6}(i)\sum_j(6x_j^5y_j-20x_j^3y_j^3+6x_jy_j^5)\ , \quad (4)$$

where $A_n^m(i)$ is the coefficient of the CEF at the ith site of the R ions. $\mathcal{H}'_{CEF}(i)$ for the R' ions is expressed by the similar equation with $A_n'^m(i)$. Some relations such as $A_2^{-2}(1)=-A_2^{-2}(2)$, $A_2^{-2}(3)=-A_2^{-2}(4)$, $H_m(1)$

$=H_m(2)$, and $H_m(3)=H_m(4)$, etc., hold because of the crystal symmetry. For simplicity we further assume here that $A_n^m(1)=A_n^m(4)$, $A_n^m(2)=A_n^m(3)$, $H_m(1)=H_m(4)$, and $H_m(2)=H_m(3)$, etc., neglecting the difference between f and g sites. Thus the molecular field H_m is assumed to be independent of the site. The total magnetization is determined from the condition that the total free energy [Eq. (1)] should be minimum with respect to the polar angles θ_{Fe} and ϕ_{Fe} of $\mathbf{m}_{\mathrm{Fe}}$. This procedure is repeated for different values of $\mathbf{H}$ at a given temperature T, and finally one magnetization isotherm is obtained. The temperature dependence of K_{Fe} and $m_{\mathrm{Fe}}(\equiv|\mathbf{m}_{\mathrm{Fe}}|)$ are assumed to be similar to those in $Y_2Fe_{14}B$ with a modification due to the difference in the Curie temperature T_C. We also assume that molecular-field vectors $\mathbf{H}_m(T)$ and $\mathbf{H}'_m(T)$ are antiparallel and proportional to the Fe moment vector $\mathbf{m}_{\mathrm{Fe}}(T)$. Adjustable parameters for the calculation are H_m and H'_m (the magnitude of $\mathbf{H}_m$ and $\mathbf{H}'_m$ at 0 K) and CEF parameters A_n^m and $A_n'^m$ for R and R' ions at the f_1 site.

We have calculated the magnetization curves of the $(Nd_{1-x}Dy_x)_2Fe_{14}B$ system by setting $R=$Nd and $R'=$Dy. For A_n^m and H_m, we adopted the values of $Nd_2Fe_{14}B$ given in Ref. 6. As for the $Dy_2Fe_{14}B$ parameters, on the other hand, we found that H'_m (=145 K) given in Ref. 6 is too small to reproduce the present magnetization curves in field of up to 300 kOe. We adjusted the value of H'_m so as to fit these curves using the same CEF parameters $A_n'^m$ as those in Ref. 6 and obtained the value $H'_m=180$ K. The CEF and molecular-field parameters used are presented in Table I. This set of parameters is not a unique one which reproduces the experiment. For example, we have already pointed out[16] that, in the $R_2Fe_{14}B$ compounds with heavy R, magnetization curves can be fitted without including the sixth-order CEF terms. The 0-K value of K_{Fe} we adopted here is $K_{\mathrm{Fe}}(0)=0.86$ K. As for $m_{\mathrm{Fe}}(0)$, we used the different values for the two end members, namely, $2.20\mu_B$ for $Nd_2Fe_{14}B$ and $2.24\mu_B$ for $Dy_2Fe_{14}B$, which were determined independently so as to reproduce the observed magnetization of each compound. We have then assumed that the $m_{\mathrm{Fe}}(0)$ value in the mixed composition is given by the linear interpolation using the two values. The calculated magnetization curves at 4.2 and 290 K are shown in Figs. 1 and 3, respectively, in comparison with the observed ones. In these calculations we included the first-excited J multiplet of the Nd ion in $\mathcal{H}_R$, while only the ground J multiplet was taken into account for the Dy ion in $\mathcal{H}_{R'}$. The formulation including the excited J multiplets has been described in Ref. 6 in detail. We have also confirmed that, in $(Nd_{1-x}Dy_x)_2Fe_{14}B$, the influence of the excited J multiplets appears evidently in magnetization curve especially near FOMP as reported in $R_2Fe_{14}B$ compounds with $R=$Pr, Nd, and Sm.[6] As seen in Fig. 1, a general trend of the observed curves including FOMP is well reproduced by the calculation. Solid lines in Fig. 2 indicate the calculated values of H_j, ΔM, M_0, and θ as a function of x. The agreement with the observations are remarkable especially for H_j and M_0.

As discussed in Ref. 6, the FOMP in $Nd_2Fe_{14}B$ is ascribed to the double minimum shape of the free energy as a function of the angle between the field and moment direction, which is caused mainly by the higher-order CEF potentials of the Nd ions. An effect of R-Fe exchange interactions is also important in FOMP. In the field applied along the hard direction, large Fe moments ($28m_{\mathrm{Fe}}$) with small anisotropy ($28K_{\mathrm{Fe}}$) easily tend to rotate to the field direction so as to gain the Zeeman energy. Through the ferromagnetic Nd-Fe interaction, this motion will help the rotation of the Nd moment, which is strongly confined to its easy direction owing to the CEF interaction. As mentioned above, H_j decreases with increasing x in the diluted systems $(Nd_{1-x}Y_x)_2Fe_{14}B$ and $(Nd_{1-x}La_x)_2Fe_{14}B$.[12] The decrease is due to the reduction of CEF and Nd-Fe exchange energy as compared with the Zeeman energy of Fe. Namely, Nd moments rotate more easily in the diluted system, reaching the critical angle of the jump at lower fields. In the $(Nd_{1-x}Dy_x)_2Fe_{14}B$ system, on the other hand, Dy moments tend to prevent the Nd moment from rotation through the Dy-Fe and Nd-Fe interactions, since the CEF interactions for Dy ions are much larger than those for Nd ions in the present case. This model clearly explains the rapid increase in H_j with increasing x.

As shown in Fig. 2(b), the calculated value of ΔM as a function of x is in good agreement with the observed one, although the former is slightly smaller than the latter. According to this calculation, the magnetization jump will disappear around $x=0.42$, indicating that the contribution from the CEF potential of Nd ions is reduced with increasing x.

At room temperature the magnetization curves for the samples with $x=0$–1 are nicely reproduced by the calculation, as shown in Fig. 3. For the $x=1$ sample, an intersection of the easy- and hard-axis curves occurs around 290 kOe. The present calculation up to the higher field has shown that the hard-axis magnetization in $Dy_2Fe_{14}B$ does not exhibit a saturation behavior as seen in the samples with $x\leq 0.6$, but continues to increase even in the field range beyond 1000 kOe. The solid line in Fig. 4(a) is

TABLE I. CEF parameters A_n^m and molecular field H_m at 0 K used in the present calculation, where $A_n^m a_0^n/k_B$ (a_0: Bohr radius) and $H_m\mu_B/k_B$ are expressed in units of Kelvin.

	A_2^0	A_2^{-2}	A_4^0	A_4^{-2}	A_4^4	A_6^0	A_6^{-2}	A_6^4	A_6^{-6}	H_m
$Nd_2Fe_{14}B$	295	−454	−12.3	0	0	−1.84	9.80	−15.9	0	350
$Dy_2Fe_{14}B$	302	−467	−12.7	0	0	−0.973	0	−5.29	0	180

the calculated value of H_A^* as a function of x, which is in good agreement with the experiment, although the former is slightly larger than the latter. This result confirms that the rapid increase in H_A^* yields an enhancement of coercivity of the permanent magnet such as $(Nd_{1-x}Dy_x)_{15}Fe_{77}B_8$.[17] In Fig. 4(b) the calculated values of saturation magnetization along the easy and hard directions are indicated by the dashed and solid lines, respectively. The two lines are intersected between $x=0.2$ and 0.33, well reproducing the experimental results.

As for the spin-reorientation phenomena in $(Nd_{1-x}Dy_x)_2Fe_{14}B$, calculated values of θ and T_{SR} are in excellent agreement with the observed ones, as shown in Figs. 2(d) and 6, respectively. Both θ and T_{SR} gradually decrease with increasing x, because the spin tilting is caused by the competition between lower- and higher-order CEF potentials of Nd ions. The CEF potentials of Dy ions which favor the [001] direction will modify this balance. The calculation predicts that no spin reorientation will occur in the samples with $x>0.79$.

In Fig. 7 we have given the calculated temperature dependence of spontaneous magnetization $|M|$ and tilting angle θ for the compound with $x=0.125$. An anomalous increase in magnetization occurs below T_{SR}. This phenomenon was first observed in the $Nd_2Fe_{14}B$ compound by Hirosawa *et al.*[5] and also reported in the $Nd_2(Fe_{1-x}Al_x)_{14}B$ system.[18] It is also revealed by the present calculation that, in the compound with $x\leq 0.6$, the magnetic moments of Nd, Dy, and Fe are noncollinear even in zero field at low temperatures. For example, the calculated magnetic structure in the sample with $x=0.125$ is schematically shown in Fig. 8. In zero field all the moments lie in the same $(1\bar{1}0)$ plane. Because of larger uniaxial magnetic anisotropy of Dy ions, Dy moments remain nearer to the [001] direction, as compared with Nd moments. When a high field ($H=200$ kOe $>H_j$) is applied along the [100] direction, the FOMP occurs and all moments lie in the (001) plane, as shown in Fig. 8(b); the Fe moment is parallel to the [100] direction, while the Nd and Dy moments are not yet parallel to the field direction owing to the contribution from the A_2^{-2} term in the CEF potential. Such a noncollinear magnetic structure within the (001) plane in zero field has already been proposed for $R_2Fe_{14}B$ compounds with $R=$Sm, Er, Tm, and Yb and confirmed experimentally by neutron diffraction for the Tm compound.[19] Figure 9 exhibits the calculated temperature dependence of the magnitude of Nd or Dy moments and the difference in tilting angle between Fe and Nd or Dy moments for the sample with $x=0.125$. This result suggests that the anomalous increase in total magnetization below T_{SR} (Fig. 7) is due to the increase in magnetic moment of the Nd ions, since the Dy moment exhibits no anomaly. This figure also shows that the noncollinear magnetic structure persists up to T_{SR}.

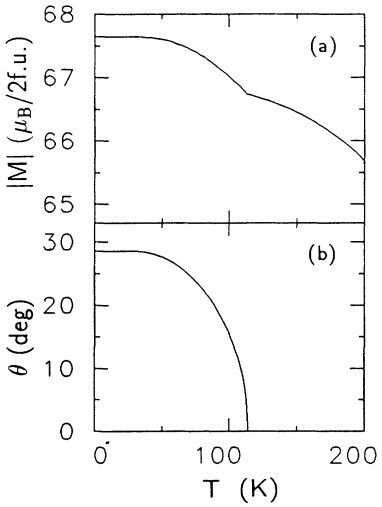

FIG. 7. Calculated temperature dependence of (a) the spontaneous magnetization $|M|$ and (b) the tilting angle θ from the [001] axis for $(Nd_{1-x}Dy_x)_2Fe_{14}B$ with $x=0.125$.

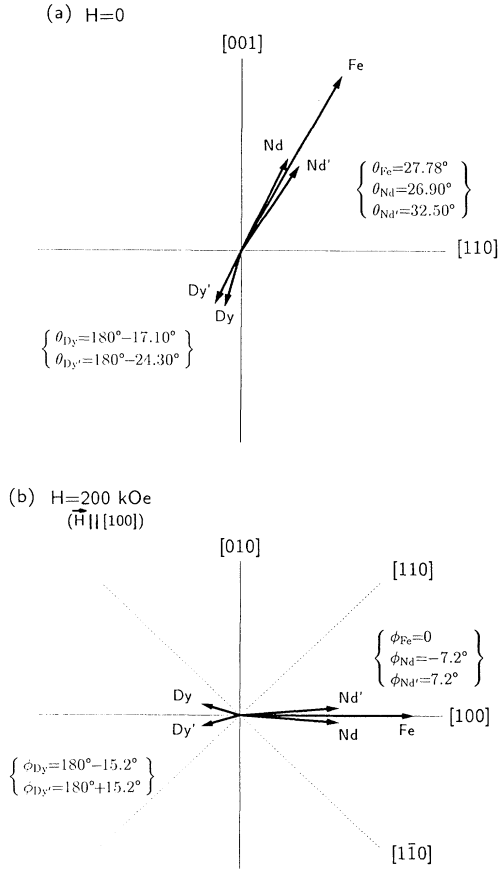

FIG. 8 Calculated magnetic structure for $(Nd_{1-x}Dy_x)_2Fe_{14}B$ with $x=0.125$ at 0 K; (a) in zero field and (b) in the field of 200 kOe applied along the [100] direction. The polar angles θ and ϕ with subscripts (Fe, Nd, and Dy) represent the direction of magnetic moment of respective ions; Nd and Dy denote those of f_1 $(=g_2)$ and Nd' and Dy' denote those of g_1 $(=f_2)$ sites.

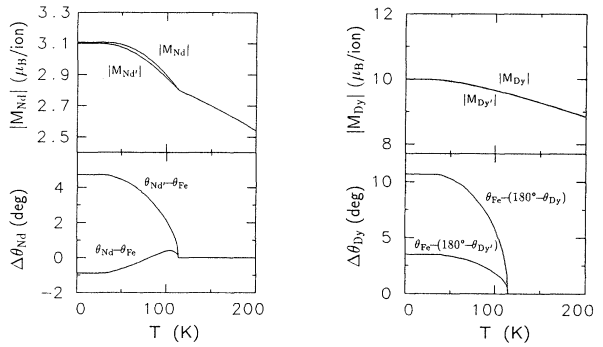

FIG. 9. Calculated temperature dependence of the magnitude of Nd or Dy moments $|M_{Nd}|$ or $|M_{Dy}|$ and the difference in tilting angle between Fe and Nd or Dy moments, $\Delta\theta_{Nd}$ or $\Delta\theta_{Dy}$, for $(Nd_{1-x}Dy_x)_2Fe_{14}B$ with $x=0.125$.

It should be noted that the real magnetic structure would be more complicated, since the magnitudes of A_n^m ($A_n'^m$) and H_m (H_m') are different for f and g sites in reality. We have performed, for some $R_2Fe_{14}B$ compounds, a detailed investigation of the effect of using different values of the parameters in f and g sites. We have then found that there is no appreciable difference in the calculated magnetization, as far as the relations $A_n^m=[A_n^m(f)+A_n^m(g)]/2$ and $H_m=[H_m(f)+H_m(g)]/2$ hold. We can thus specify that the calculated tilting angles θ_{Nd} and $\theta_{Nd'}$ given in Figs. 8 and 9 represent, respectively, the averages of $\theta_{Nd}(f_1)$ and $\theta_{Nd}(g_2)$ and those of $\theta_{Nd}(f_2)$ and $\theta_{Nd}(g_1)$. These relations are also expected to hold for the angles of Dy moments. Our simplification presented here is useful to understand the interplay of CEF potentials and R-Fe interactions, since the essential point in this system is not the difference between f and g sites, but the difference between f_1 and f_2 (or between g_1 and g_2) sites.

V. CONCLUDING REMARKS

The magnetic characteristics of $Nd_2Fe_{14}B$, such as FOMP, spontaneous magnetization, and spin reorientation, are affected by the substitution of Dy ions for Nd ions. The high-field magnetization process in $(Nd_{1-x}Dy_x)_2Fe_{14}B$ is successfully explained by the calculation based on the CEF theory including the molecular field due to Nd-Fe and Dy-Fe exchange interactions. The Nd-Dy interaction as well as the Nd-Nd and Dy-Dy interactions can be ignored in this system. The rapid increase in H_j with increasing x is mainly due to the Dy-Fe interaction and CEF interaction at Dy ions. A gradual decrease in both tilting angle and T_{SR} with increasing Dy concentration implies that the complex anisotropy of Nd ions due to higher-order terms in the CEF potential is simply diluted by Dy ions. It is concluded that the characters of the Fe sublattice are almost unaffected by the substitution of Dy ions for Nd ions.

Finally, the high reproducibility of the experimental results by the present calculation enables us to conclude that the magnetic properties of the $(R_{1-x}R_x')_2Fe_{14}B$ system can be predicted for any combination of rare-earth elements R and R'.

ACKNOWLEDGMENTS

We are much indebted to Dr. S. Hirosawa of Sumitomo Special Metals Company, Ltd., for providing us the single crystals. We also thank Dr. N. Saito for helping with the ac susceptibility measurements and staff members of High Field Laboratory of Tohoku University for the operation of the Bitter and hybrid magnets. This work was partly supported by a Grant-in-Aid for Scientific Research (C) from the Ministry of Education, Science and Culture, Japan.

[1]M. Sagawa, S. Fujimura, N. Togawa, H. Yamamoto, and Y. Matsuura, J. Appl. Phys. **55**, 2083 (1984).
[2]J. F. Herbst, J. J. Croat, F. E. Pinkerton, and W. B. Yelon, Phys. Rev. B **29**, 4176 (1984).
[3]D. Givord, H. S. Li, and J. M. Moreau, Solid State Commun. **50**, 497 (1984).
[4]D. Givord, H. S. Li, and R. Perrier de la Bathie, Solid State Commun. **51**, 857 (1984).
[5]S. Hirosawa, Y. Matsuura, H. Yamamoto, S. Fujimura, M. Sagawa, and H. Yamauchi, J. Appl. Phys. **59**, 873 (1986).
[6]M. Yamada, H. Kato, H. Yamamoto, and Y. Nakagawa, Phys. Rev. B **38**, 620 (1988).
[7]S. Kajiwara, G. Kido, Y. Nakagawa, S. Hirosawa, and M. Sagawa, J. Phys. Soc. Jpn. **56**, 826 (1987).
[8]L. Pareti, F. Bolzoni, and O. Moze, Phys. Rev. B **32**, 7604 (1985).
[9]H. Kato, M. Yamada, G. Kido, Y. Nakagawa, S. Hirosawa, and M. Sagawa, J. Phys. (Paris) Colloq. **49**, C8-575 (1988).
[10]J. M. Cadogan, J. P. Gavigan, D. Givord, and H. S. Li, J. Phys. F **18**, 779 (1988).
[11]D. Givord, H. S. Li, J. M. Cadogan, J. M. D. Coey, J. P. Gavigan, O. Yamada, H. Maruyama, M. Sagawa, and S. Hirosawa, J. Appl. Phys. **63**, 3713 (1988).
[12]D. W. Lim, H. Kato, M. Yamada, G. Kido, Y. Nakagawa, and S. Hirosawa, J. Magn. Magn. Mater. **90&91**, 72 (1990).
[13]M. Sagawa, S. Fujimura, H. Yamamoto, Y. Matsuura, and K. Hiraga, IEEE Trans. Magn. **MAG-20**, 1584 (1984).
[14]Y. Nakagawa, K. Noto, A. Hoshi, K. Watanabe, S. Miura, G. Kido, and Y. Muto, Physica B **155**, 69 (1989).
[15]M. R. Ibarra, C. Marquina, P. A. Algarabel, J. I. Arnaudas, and A. del Moral, J. Appl, Phys. **64**, 5537 (1988).
[16]M. Yamada, H. Kato, H. Hiroyoshi, H. Yamamoto, and Y. Nakagawa, J. Magn. Magn. Mater. **70**, 328 (1987).
[17]Y. Nakagawa, H. Hiroyoshi, M. Sagawa, S. Hirosawa, and K. Tokuhara, IEEE Trans. Magn. **MAG-23**, 2530 (1987).
[18]M. C. D. Deruelle, M. Yamada, H. Yamauchi, and Y. Nakagawa, Phys. Rev. B **42**, 10 291 (1990).
[19]M. Yamada, Y. Yamaguchi, H. Kato, H. Yamamoto, and Y. Nakagawa, Solid State Commun. **56**, 663 (1985).